Acta Crystallographica Section C
Crystal Structure Communications
ISSN 0108-2701

Aripiprazole salts. II. Aripiprazole perchlorate

Eleonora Freire,[a,b]*‡ Griselda Polla[a] and Ricardo Baggio[a]

[a]Gerencia de Investigación y Aplicaciones, Centro Atómico Constituyentes, Comisión Nacional de Energía Atómica, Buenos Aires, Argentina, and [b]Escuela de Ciencia y Tecnología, Universidad Nacional General San Martín, Buenos Aires, Argentina
Correspondence e-mail: freire@tandar.cnea.gov.ar

Received 20 April 2012
Accepted 10 May 2012
Online 18 May 2012

The molecular structure of aripiprazole perchlorate (systematic name: 4-(2,3-dichlorophenyl)-1-{4-[(2-oxo-1,2,3,4-tetrahydroquinolin-7-yl)oxy]butyl}piperazin-1-ium perchlorate), $C_{23}H_{28}Cl_2N_3O_2^+\cdot ClO_4^-$, does not differ substantially from the recently published structure of aripiprazole nitrate [Freire, Polla & Baggio (2012). *Acta Cryst.* C**68**, o170–o173]. Both compounds have almost identical bond distances, bond angles and torsion angles. The two different counter-ions occupy equivalent places in the two structures, giving rise to very similar first-order 'packing motifs'. However, these elemental arrangements interact with each other in different ways in the two structures, leading to two-dimensional arrays with quite different organizations.

Comment

Aripiprazole (Arip, 7-{4-[4-(2,3-dichlorophenyl)-1-piperazinyl]butoxy}-3,4-dihydroquinolin-2(1*H*)-one) is an antipsychotic drug, perhaps the most relevant representative of a modern family of atypical antipsychotics (Travis *et al.*, 2005), with a different therapeutic activity from those of the classical antipsychotic drugs in standard use.

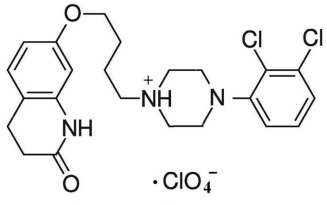

(I)

The drug crystallizes in a number of polymorphic and solvatomorphic varieties, described in a large number of patents, but the structural information provided is far from complete, and when their X-ray powder diffraction (XRPD) diagrams are reported they usually only fulfil the role of fingerprint identifiers. The main source of structural information on Arip compounds consists of a paper by Tessler & Goldberg (2006), complemented by two excellent works by Braun *et al.* (2009*a*,*b*). In the first of these latter works, Braun and coworkers report a number of different forms of the Arip molecule in its free form, included in the Cambridge Structural Database (CSD; Allen, 2002) with refcodes MELFIT01–05, while in the second of these latter works they present different solvates, *viz.* refcodes MELFEP01 (ethanol solvate), MELFOZ01 (methanol solvate), MELFUF01 (monohydrate) and MOXDAF01 (1,2-dichloroethane solvate).

With Arip salts, the situation is slightly different, and even if some of them have been described in the patent literature, no structure of an Arip salt had been described until recently, namely aripiprazole nitrate, (II) (Freire *et al.*, 2012). The protonated state of the ligand confers interesting properties on the structure, which prompted us to analyse other AripH$^+$ salts. We report herein a second AripH$^+$ salt, namely aripiprazole perchlorate or AripH$^+\cdot ClO_4^-$, (I).

Compound (I) (Fig. 1) consists of an AripH$^+$ cation and a ClO_4^- counter-ion, completing the structure and providing charge balance. The whole AripH$^+\cdot ClO_4^-$ molecular assembly in (I) is very similar to that in the nitrate counterpart, (II), in terms of bond lengths, bond angles and torsion angles, and reference should be made to the detailed description in Freire *et al.* (2012). As a measure of these similarities, the least-squares fit of the cations of both structures leads to a mean deviation of 0.23° (Fig. 2), and even the (relatively free) counter-ions, not involved in the fitting, sit in almost exactly the same place, their baricentres lying only 0.52 Å apart.

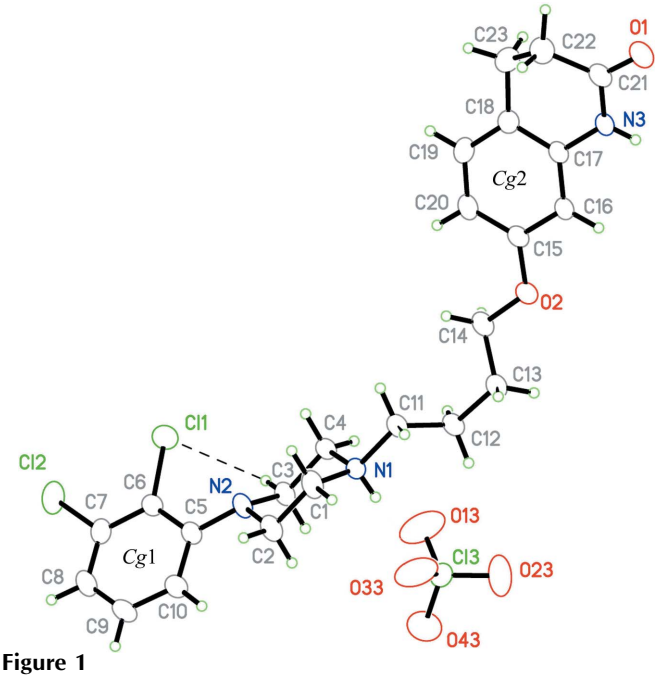

Figure 1
The asymmetric unit of (I), showing the atom-numbering scheme. Ring centroids are labelled. Displacement ellipsoids are drawn at the 40% probability level. The dashed line represents the intramolecular C—H···Cl interaction.

‡ Member of Consejo Nacional de Investigaciones Científicas y Técnicas, Conicet.

 doi:10.1107/S0108270112021348

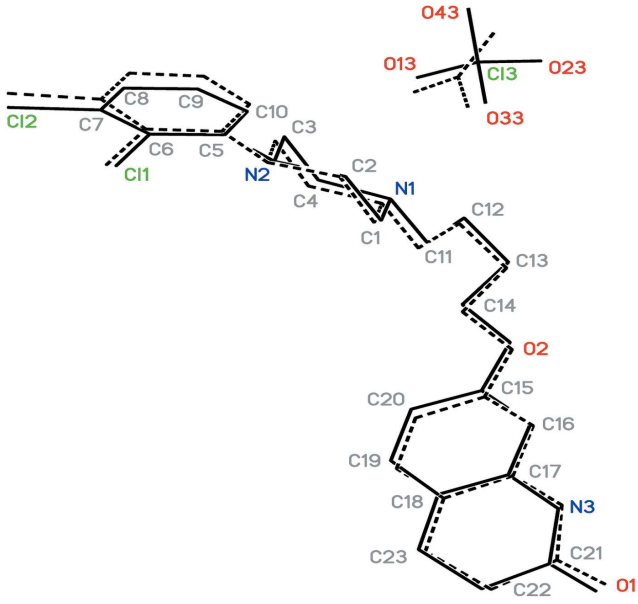

Figure 2
A comparison of the stereodisposition of perchlorate salt (I) (solid lines) and nitrate salt (II) (dashed lines). Note the slight shift between the counter-ions.

If the noncovalent interactions defining the spatial arrangement of (I) (hydrogen bonds are given in Table 1 and π bonds are given in Table 2) are compared with those in nitrate isologue (II), it can be seen that all main interactions are present, in particular the hydrogen bonds involving the N—H donors (Table 1, entries 2 and 3). These hydrogen bonds give rise to similar 'first-order' packing motifs [point (*a*) below], which in turn act as building blocks of fairly different structures [point (*b*) below].

The first entry in Table 1 corresponds to an intramolecular C—H···Cl interaction characteristic of the dichlorophenylpiperazin-1-yl group in all reported Arip variants, being in (I), as it was in (II), rather unexceptional.

(*a*) The second entry in Table 1, the strong hydrogen bond between the amide groups of adjacent Arip molecules, is characteristic of most of the reported Arip variants, though leading to different supramolecular synthons, *viz.* a catemer [graph-set $C(4)$] or a diamide $R_2^2(8)$ dimer [this was discussed in detail in Freire *et al.* (2012); for graph-set nomenclature, see Bernstein *et al.* (1995)].

In the cases of (I) and (II), this hydrogen bond leads to almost identical catemers (zones labelled **A** in Fig. 3), running along the shortest axis in each case [*b* in (I) and *a* in (II)]. There is, however, an important structural difference between the two cases, in that the translation symmetry operations relating concatenated moieties in these catemers are the *Pbca* *a*-glide plane in (II) but the $P2_1/c$ 2_1 axis in (I), while having very similar translation 'steps' of 4.2322 (2) and 4.1552 (3) Å, respectively.

Contrasting with the previous interaction, which is common to almost all Arip compounds, the second N—H···O bond is instead unique to (I) and (II), as some of the main participants (the perchlorate/nitrate counter-ions as acceptors, and the extra H1 atom as donor) are present only in these salts. Even

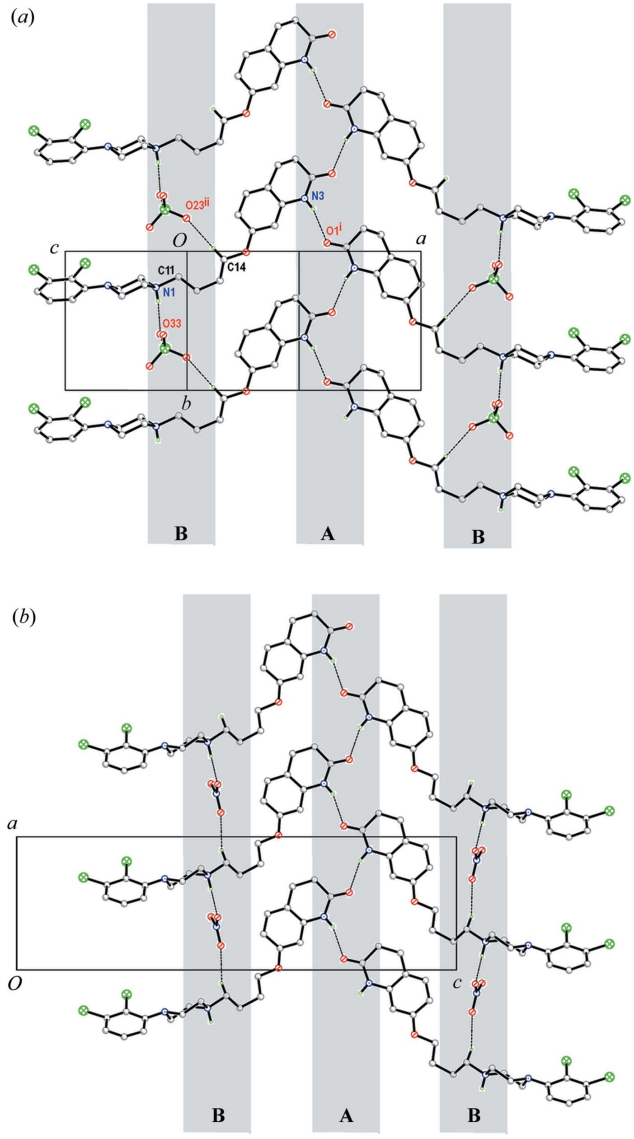

Figure 3
Packing diagrams for (*a*) (I), projected on (401), and (*b*) (II), projected on (010). Dashed lines indicate hydrogen bonds. The shaded regions **A** and **B** correspond to different hydrogen-bonding regimes, as discussed in the *Comment*. [Symmetry codes: (i) $-x+2, y+\frac{1}{2}, -z+\frac{3}{2}$; (ii) $x, y-1, z$.]

though the molecular strips are common building blocks in most Arip structures, in the present case this second interaction strengthens their mutual link and enhances their internal cohesion, forming a rather different entity (Fig. 3). In fact, zones **B** in Fig. 3 show the contribution of both counter-ions to the stability of the elementary packing units therein depicted. Both include the second strong N—H···O synthon (Table 1, third entry), identical in both structures, and a second, weak, C—H···O hydrogen bond which serves as an effective link between second neighbours in the catemer. However, these are characteristic of each structure, involving C11—H11 in (II) and C14—H14 in (I), a difference which is probably due to the geometric differences between the anions (planar nitrate *versus* tetrahedral perchlorate). In spite of these differences, the 'first-order' packing motifs shown in Fig. 3 are very similar.

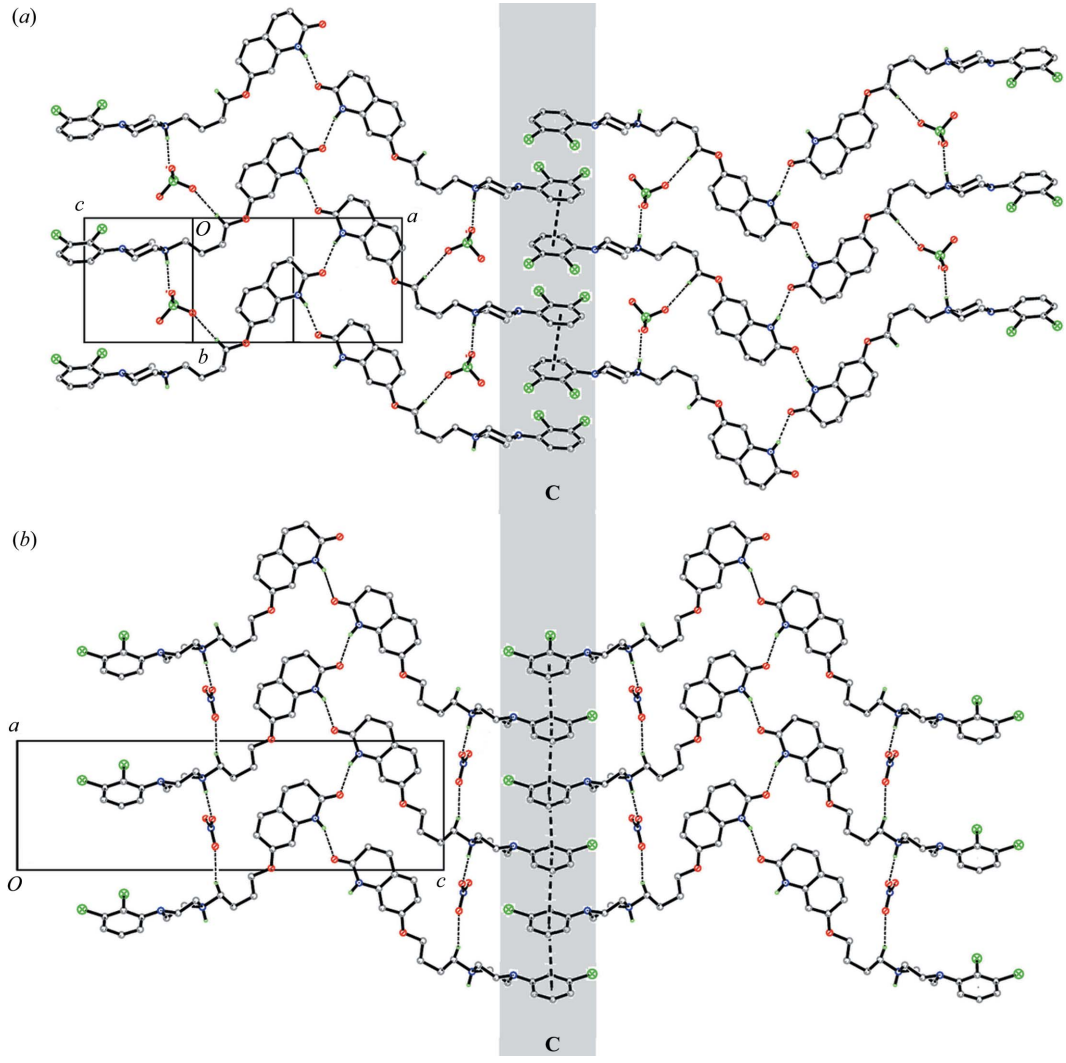

Figure 4
The same views as in Fig. 3 for (*a*) (I) and (*b*) (II), but showing the lateral interactions (dashed lines) between the structures shown therein. The shaded region **C** is discussed in the *Comment*.

(*b*) Finally, these motifs further interact laterally, *via* π–π bonds (shaded region **C** in Fig. 4), but here also there are significant crystallographic differences. In the case of (II), the process is achieved through an (x, y, z + 1) translation of the whole group or, in other words, the interdigitation of aromatic rings in neighbouring cells, adjacent along c (Fig. 4*b*). These π–π interactions result in the formation of a continuous thread along [100], and the two-dimensional structure generated by juxtaposition of the broad [100] bands ends up being an array parallel to (010).

In contrast, the π–π linkage process in (I) is noticeably more complicated, generated by the $P2_1/c$ c glide (which provides an $[00\frac{1}{2}]$ translation) in combination with a further lateral [2,0,0] shift of the resulting image (Fig. 4*a* and Table 2). These two translational effects combine to give an alternating π–π approach (Fig. 4*a*) and the consequence is a two-dimensional structure parallel to (401). In summary, the two-dimensional repeat pattern consists of two molecular ribbons parallel to [100] in (II) but four ribbons parallel to [010] in (I).

There are also differences in the planarity of these two two-dimensional arrays. When viewed in projection, that in (II) appears noticeably undulating (Fig. 5*b*; largest deviation from the mean plane ∼5 Å), consistent with the fact that the linkage operator at **A** is a plane (shown as a dashed line) and which allows for the 'mirror-like' aspect shown therein by the two-dimensional trace. In contrast, the 2_1 axis in (I) forces a linear disposition and thus favours a more planar set-up, with a maximum deviation from the mean plane of ∼2 Å (Fig. 5*a*). Regarding packing efficiency, the corrugated scheme in nitrate salt (II) seems to be more efficient than the more planar scheme in perchlorate salt (I), where a significant increase of 6% in molecular weight leads to a mere increase of 2% in density.

The remaining interactions presented in Tables 1 and 2 are noticeably weaker and provide interplanar interactions.

The results presented herein suggest that there are spatial arrangements in AripH$^+$ salts (*viz.* those shown in Fig. 3) which behave as fairly stable motifs. They do not seem to

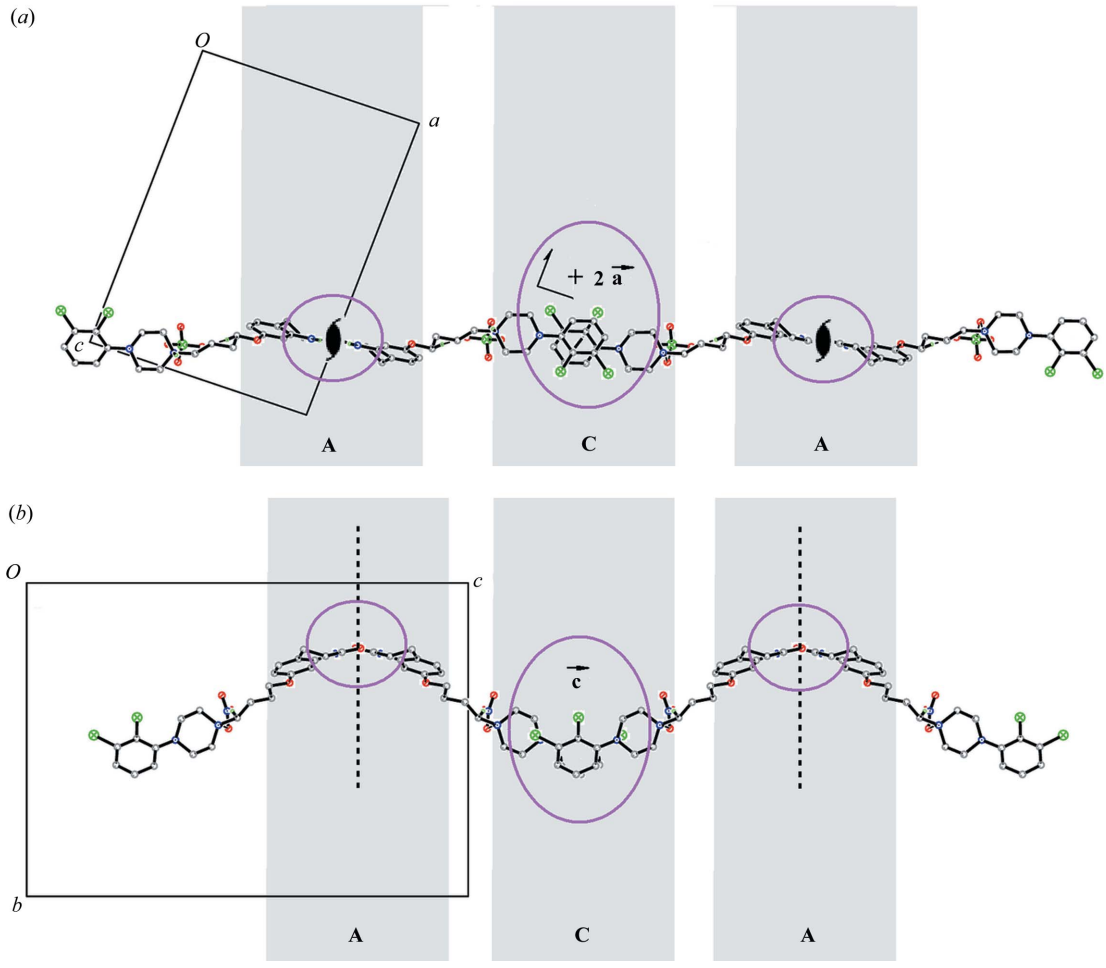

Figure 5
Packing diagrams for (*a*) (I) and (*b*) (II), at right angles to those shown in Fig. 4. The circled areas indicate the symmetry operations giving rise to the packing linkage.

depend on the symmetry or counter-ion, and can act as well defined building blocks for more complex packing set-ups. This presumed stability should be confirmed through further systematic work on aripiprazole salts, a research line on which we are presently engaged.

Experimental

Aripiprazole (67 mg, 0.15 mmol) was dissolved in a boiling mixture of methanol (5 ml) and acetone (0.5 ml). When dissolution was complete, an excess of concentrated $HClO_4$ was added dropwise and the resulting solution left to cool slowly. Excellent crystals of $AripH^+\cdot ClO_4^-$, (I), in the form of colourless prisms, appeared within a few hours and were used as obtained without further recrystallization.

Crystal data

$C_{23}H_{28}Cl_2N_3O_2^+\cdot ClO_4^-$
M_r = 548.83
Monoclinic, $P2_1/c$
a = 14.7348 (5) Å
b = 8.3103 (3) Å
c = 20.1590 (7) Å
β = 92.557 (3)°
V = 2466.03 (16) Å^3
Z = 4
Mo $K\alpha$ radiation
μ = 0.42 mm^{-1}
T = 291 K
0.24 × 0.16 × 0.14 mm

Data collection

Oxford Gemini S Ultra CCD area-detector diffractometer
Absorption correction: multi-scan (*CrysAlis PRO*; Oxford Diffraction, 2009)
T_{min} = 0.92, T_{max} = 0.94
11131 measured reflections
5590 independent reflections
4186 reflections with $I > 2\sigma(I)$
R_{int} = 0.022

Refinement

$R[F^2 > 2\sigma(F^2)]$ = 0.048
$wR(F^2)$ = 0.121
S = 1.03
5590 reflections
324 parameters
H atoms treated by a mixture of independent and constrained refinement
$\Delta\rho_{max}$ = 0.39 e Å^{-3}
$\Delta\rho_{min}$ = −0.35 e Å^{-3}

Table 1
Hydrogen-bond geometry (Å, °).

*Cg*2 is the centroid of the C15–C20 benzene ring.

D—H···A	D—H	H···A	D···A	D—H···A
C3—H3B···Cl1	0.97	2.57	3.193 (2)	122
N3—H3···O1^{i}	0.81 (3)	2.20 (3)	2.985 (3)	162 (2)
N1—H1···O33	0.83 (3)	2.05 (3)	2.875 (3)	174 (3)
C14—H14A···O23^{ii}	0.97	2.45	3.413 (4)	175
C1—H1A···O23^{iii}	0.97	2.51	3.441 (4)	160
C4—H4B···Cg2^{iii}	0.97	2.81	3.541 (2)	133

Symmetry codes: (i) $-x+2, y+\frac{1}{2}, -z+\frac{3}{2}$; (ii) $x, y-1, z$; (iii) $-x+1, -y+1, -z+2$.

Table 2
π–π and halogen–π contacts (Å, °).

*Cg*1 is the centroid of the C5–C10 benzene ring, ccd is the centroid-to-centroid distance, cpd is the centroid-to-plane distance and sa is the slippage angle (angle subtended by the intercentroid vector to the plane normal). For details, see Janiak (2000).

Group 1/Group 2	ccd (Å)	cpd (Å)	sa (°)
$Cg1\cdots Cg1^{i}$	3.7751 (14)	3.536	20.48
$Cl1\cdots Cg1^{i}$	3.5481 (12)	3.474	11.75

Symmetry code: (i) $-x, -y, -z+2$.

All H atoms were found in a difference map. H atoms attached to N atoms were further refined, giving N—H = 0.81 (3)–0.83 (3) Å and U_{iso}(H) = 0.037 (7)–0.040 (7) Å^2. H atoms attached to C atoms were idealized and allowed to ride, with methylene C—H = 0.97 Å and aromatic C—H = 0.93 Å, and with U_{iso}(H) = 1.2U_{eq}(C).

Data collection: *CrysAlis PRO* (Oxford Diffraction, 2009); cell refinement: *CrysAlis PRO*; data reduction: *CrysAlis PRO*; program(s) used to solve structure: *SHELXS97* (Sheldrick, 2008); program(s) used to refine structure: *SHELXL97* (Sheldrick, 2008); molecular graphics: *SHELXTL* (Sheldrick, 2008); software used to prepare material for publication: *SHELXL97* and *PLATON* (Spek, 2009).

The provision of aripiprazole by Laboratorios Maprimed is gratefully acknowledged. The authors also acknowledge ANPCyT (project No. PME 2006-01113) for the purchase of the Oxford Gemini CCD diffractometer, and the Spanish Research Council (CSIC) for the provision of a free-of-charge licence to the Cambridge Structural Database (Allen, 2002).

Supplementary data for this paper are available from the IUCr electronic archives (Reference: SK3436). Services for accessing these data are described at the back of the journal.

References

Allen, F. H. (2002). *Acta Cryst.* B**58**, 380–388.
Bernstein, J., Davis, R. E., Shimoni, L. & Chang, N.-L. (1995). *Angew. Chem. Int. Ed. Engl.* **34**, 1555–1573.
Braun, D. E., Gelbrich, T., Kahlenberg, V., Tessadri, R., Wieser, J. & Griesser, U. (2009*a*). *J. Pharm. Sci.* **98**, 2010–2026.
Braun, D. E., Gelbrich, T., Kahlenberg, V., Tessadri, R., Wieser, J. & Griesser, U. (2009*b*). *Cryst. Growth Des.* **9**, 1054–1065.
Freire, E., Polla, G. & Baggio, R. (2012). *Acta Cryst.* C**68**, o170–o173.
Janiak, C. (2000). *J. Chem. Soc. Dalton Trans.* pp. 3885–3896.
Oxford Diffraction (2009). *CrysAlis PRO*. Oxford Diffraction Ltd, Yarnton, Oxfordshire, England.
Sheldrick, G. M. (2008). *Acta Cryst.* A**64**, 112–122.
Spek, A. L. (2009). *Acta Cryst.* D**65**, 148–155.
Tessler, L. & Goldberg, I. (2006). *J. Inclusion Phenom. Macrocycl. Chem.* **55**, 255–261.
Travis, M. J., Burns, J., Dursun, S., Faby, T., Frangou, S., Gray, R., Haddad, P. M., Hunter, R., Taylor, D. M. & Young, A. H. (2005). *Int. J. Clin. Pract.* **59**, 485–495.